The Journal of Infectious Diseases

MAJOR ARTICLE

Therapeutic Implications of Human Umbilical Cord Mesenchymal Stromal Cells in Attenuating Influenza A(H5N1) Virus–Associated Acute Lung Injury

Hayley Loy,[1] Denise I. T. Kuok,[1] Kenrie P. Y. Hui,[1] Miranda H. L. Choi,[2] W. Yuen,[2] John M. Nicholls,[3] J. S. Malik Peiris,[1] and Michael C. W. Chan[1]

[1]School of Public Health, Li Ka Shing Faculty of Medicine, University of Hong Kong, Hong Kong Special Administrative Region, China; [2]Healthbaby Biotech, Hong Kong Special Administrative Region, China; and [3]Department of Pathology, Li Ka Shing Faculty of Medicine, University of Hong Kong, Hong Kong Special Administrative Region, China

Background. Highly pathogenic avian influenza viruses can cause severe forms of acute lung injury (ALI) in humans, where pulmonary flooding leads to respiratory failure. The therapeutic benefits of bone marrow mesenchymal stromal cells (MSCs) have been demonstrated in a model of ALI due to influenza A(H5N1) virus. However, clinical translation is impractical and limited by a decline in efficacy as the age of the donor increases. Umbilical cord MSCs (UC-MSCs) are easier to obtain by comparison, and their primitive source may offer more-potent therapeutic effects.

Methods. Here we investigate the therapeutic efficacy of UC-MSCs on the mechanisms of pulmonary edema formation and alveolar fluid clearance and protein permeability of A(H5N1)-infected human alveolar epithelial cells. UC-MSCs were also tested in a mouse model of influenza ALI.

Results. We found that UC-MSCs were effective in restoring impaired alveolar fluid clearance and protein permeability of A(H5N1)-infected human alveolar epithelial cells. UC-MSCs consistently outperformed bone marrow MSCs, partly because of greater growth factor secretion of angiopoietin 1 and hepatocyte growth factor. Conditioned UC-MSC medium and UC-MSC exosomes were also able to recapitulate these effects. However, UC-MSCs only slightly improved survival of A(H5N1)-infected mice.

Conclusions. Our results suggest that UC-MSCs are effective in restoring alveolar fluid clearance and protein permeability in A(H5N1)-associated ALI and confer functional in addition to practical advantages over conventional bone marrow MSCs.

Keywords. Mesenchymal stromal cells; influenza; H5N1; acute lung injury.

Fatality due to highly pathogenic avian influenza A virus infection in humans is often associated with severe forms of acute lung injury (ALI). Damage to the epithelial barrier of the pulmonary alveolus causes accumulation of protein-rich edema fluid in the lumen, compromising gaseous exchange and ultimately resulting in respiratory failure [1]. Under normal physiological conditions, the depth of the alveolar lining fluid is maintained through the movement of ions through transporters that draw water from the alveolus into pulmonary interstitium through a process known as alveolar fluid clearance (AFC) [2]. The integrity of the alveolar epithelium is also essential to prevent influx of protein-rich fluid from the plasma, as well as inflammatory cells, measured by alveolar protein permeability (APP). Impairment of AFC and APP in patients with severe influenza virus infection are primary mechanisms that drive pulmonary edema formation in ALI [3].

Mesenchymal stromal cells (MSCs) are a population of multipotent cells that possess immunomodulatory properties and secrete trophic growth factors to regulate pulmonary microenvironment [4]. Recently, we showed that bone marrow MSCs (BM-MSCs) can restore impaired AFC and APP of influenza A(H5N1) virus–infected alveolar epithelial cells (AECs) [5]. Although the therapeutic effects of BM-MSCs have been well demonstrated in various ALI models [6], the decline in function with the increase in donor age limits clinical application [7]. Additionally, impracticalities such as invasive harvesting procedures, long expansion times, and low isolation yields [8] prompt the need to investigate MSCs isolated from other tissues. Perinatal tissues such as the amnion, placenta, and umbilical cord are rich sources of MSCs, and they are becoming increasingly popular for allogeneic therapy, because they share some characteristics with embryonic stem cells, suggesting that they are more primitive and of greater therapeutic potential than MSCs isolated from adult tissues [9]. Comparison studies have shown that umbilical cord MSCs (UC-MSCs) in particular have significantly higher proliferation rates, immunomodulatory capacities [10, 11], growth factor secretion [12], and antiinflammatory effects [13]. There are also less practical disadvantages associated with isolation of UC-MSCs, because the umbilical cords are more easily accessible and because the isolation procedure does not carry any risk to the donor.

Received 20 June 2018; editorial decision 27 July 2018; accepted 31 July 2018; published online August 2, 2018.

Presenting in part: Options IX for the Control of Influenza, Chicago, Illinois, 24–28 August 2016; Cytokines 2017, Kanazawa, Japan, 29 October–2 November 2017.

Correspondence: M. C. W. Chan, PhD, L6-39, Laboratory Block, Faculty of Medicine Bldg, 21 Sassoon Rd, Pokfulam, Hong Kong SAR, China (mchan@hku.hk).

DOI: 10.1093/infdis/jiy478

Several therapeutic constituents of the MSC secretome, such as conditioned medium, growth factors, and extracellular vesicles, have also been shown to be as effective as the cell they are derived from in alleviating ALI and other lung diseases [14–16], which contribute to the generation of cell-free therapy options. Exosomes (diameter, 30–100 nm) are the smallest type of extracellular vesicle constitutively secreted by all cell types as a means of cellular communication. Their cargo includes proteins, lipids, messenger RNA (mRNA), and microRNA (miRNA) that can be transferred to recipient cells. A very recent study has shown that extracellular vesicles including exosomes reduced viral replication in an influenza-associated ALI swine model [17].

Here we investigate the efficacy of UC-MSCs, using in vitro and in vivo models of ALI induced by A(H5N1) infection. The potential therapeutic effects of conditioned UC-MSC medium and UC-MSC–derived exosomes on impaired AFC and APP in vitro were also studied.

MATERIALS AND METHODS

Human MSCs

BM-MSCs were obtained and cultured as previously described [5]. UC-MSCs were isolated by HealthBaby Biotech (Hong Kong) and cultured in low-glucose (concentration 1.0 g/L) Dulbecco's modified Eagle's medium (lgDMEM) supplemented with 10% HyClone fetal bovine serum (FBS), and 1% penicillin and streptomycin was used for cell culture. Both MSC populations were cultured in a humidified atmosphere (37°C and 5% CO_2), with growth medium changed every 48 hours. Cells were detached for subculture by trypsin and seeded for experimental use upon 70% confluency. Surface marker expression was analyzed by flow cytometry to meet the minimal criteria for defining MSCs proposed by the International Society for Cell and Gene Therapy, as detailed by Chan et al [5]. Passage 4–5 MSCs were used in all experiments, and growth medium was changed to 0% serum before incubation with infected alveolar epithelial cells.

Human AECs

AECs were isolated from resected, nonmalignant lung tissue obtained from the Department of the Cardiothoracic Surgery, Queen Mary Hospital, University of Hong Kong, and cultured as previously described [18] and detailed in the Supplementary Materials, with ethics approval from the University of Hong Kong and the Hospital Authority (Hong Kong West) institutional review board.

Influenza A Virus and Infection

Influenza A/HongKong/483/97(H5N1) was used to model highly pathogenic avian influenza A virus infection. Virus stocks were grown and propagated in Madin-Darby canine kidney cells and were titered by the plaque assay and the 50% tissue culture infective dose ($TCID_{50}$) assay. All experiments were performed in a biosafety level 3 facility at the University of Hong Kong.

In Vitro Lung Injury Model

Human AECs were seeded on the apical chamber of 24-well Transwell inserts (pore diameter, 0.4 μM; Corning) at 1×10^5 cells/well with 1×10^5 BM-MSCs or UC-MSCs in the basal compartment without cell contact as previously described [19] and detailed in the Supplementary Materials.

Mouse Studies

Female BALB/C mice aged 6–8 weeks were intranasally inoculated with 10^6 log $TCID_{50}$ of A/Hong Kong/486/1997(H5N1) in 25 μL. At day 5 after infection, mice were injected intravenously with 5×10^5 UC-MSCs or National Institutes of Health 3T3 mouse embryo fibroblasts (ATCC) in 100 μL. Survival and body weight were monitored for 18 days. At days 7 and 10 after infection, virus was titrated in 3 mouse lungs per group (MSC vs fibroblast treatment groups). Bronchoalveolar lavage fluid was collected on day 7 after infection for a cytokine assay. At days 7, 10, and 14 after infection, 3 mice per group were euthanized, and the level of Evans blue dye was measured as an indicator of fluid leakage into the alveolus. Three mouse lungs per group were fixed for histopathologic analysis at day 10 after infection. The animal infection experiments were approved by the Committee on the Use of Live Animals in Teaching and Research of the University of Hong Kong (CULATR 3445-14).

AFC and APP

Fluorescein isothiocyanate (FITC)–dextran (Sigma) was used to measure of AFC and APP as described previously [5]. Briefly, the net AFC per hour was calculated as [1 − (initial apical concentration)/(final apical concentration) × (volume in μL of FITC-dextran added) × (area in cm^2 of the Transwell)]. The net APP was measured as the final basal concentration divided by the initial apical concentration and expressed as the percentage change in FITC-dextran permeability.

Preparation of Conditioned MSC Medium

AECs in Transwells were infected at a multiplicity of infection of 2 with BM-MSCs or UC-MSCs in the basal compartment. At 24 hours after infection, MSC supernatant was collected and filtered through a 100-kDa–pore filter (Millipore) and stored at −80°C until use.

Exosome Isolation

At 60% confluency, UC-MSCs were washed 3 times with Hank's balanced salt solution to remove HyClone FBS and was replenished with 10% exosome-depleted FBS lgDMEM. Supernatant was collected by passing through a 0.22-μM–pore filter at 48 hours and stored at −20°C until exosome isolation. Supernatant was thawed gently on ice and used to isolate the exosome by filtration, using the ExoEasy Maxi Kit (Qiagen), or by precipitation, using the miRCURY Exosome Isolation Kit (Exiqon), according to manufacturer's instructions.

Statistical Analyses

Mean values from 3 independent experiments were compared by 1- or 2-way analysis of variance with a post hoc Bonferroni test as appropriate. Differences were considered significant at a *P* value of <.05. All statistical analyses were performed using GraphPad Prism, version 5.0 for Windows. Survival and body weight loss among mice in MSC and fibroblast treatment groups were compared in 3 independent experiments, using the log-rank test and a linear regression model.

RESULTS

UC-MSCs Are Effective in Correcting Impaired AFC and APP of A(H5N1)-Infected Human AECs

First, we assessed the effects of UC-MSC on A(H5N1)-infected AECs in an in vitro lung injury model. The AFC rate of infected AECs decreased to a minimum 24 hours after infection but was largely restored by UC-MSCs (Figure 1A). BM-MSCs also restored the AFC rate, but the restoration was less effective than that for UC-MSCs. At 24 hours after infection, A(H5N1) infection caused a great increase in the APP of AECs. Similar to the AFC, UC-MSCs prevented a change in the APP to a greater extent than BM-MSCs (Figure 1B). The phosphate-buffered saline control has no effect on either the AFC or APP of infected AECs. We found that UC-MSCs exerted more-potent restoration effects on the AFC and APP in a cell-number-dependent manner (Supplementary Figure 1).

UC-MSCs Reduce A(H5N1)-Induced Downregulation of Ion Transporters

AFC is driven by vectorial movement of ions through epithelial transporters, which creates an osmotic gradient for water to exit the alveolar lumen [20]. AEC ion transporters are downregulated during influenza virus infection, so we studied the effect of UC-MSCs on gene expression of the epithelial Na^+ channel (ENaC), Na^+,K^+-ATPase, and cystic fibrosis transmembrane conductance regulator (CFTR) in infected AECs 24 hours after infection. Consistent with our previous studies, A(H5N1) infection significantly decreased expression of the genes encoding CFTR and subunits of ENaC and Na^+,K^+-ATPase. This was prevented by UC-MSCs, with ENaC and Na^+,K^+-ATPase subunit expression returning to at least 50% of the value for the mock-infected control, and CFTR expression was almost completely restored to the level for the mock-infected control (Figure 2A). BM-MSCs also restored ion transporter gene expression but not as effectively as UC-MSCs. Accordingly, protein expression of α1-Na^+,K^+-ATPase and CFTR was greater in A(H5N1)-infected AECs with UC-MSCs, compared with infected AECs alone or with BM-MSCs (Figure 2B).

UC-MSCs Are Potent in Regulating Inflammatory Responses of A(H5N1)-Infected AECs

A(H5N1) infection causes excessive cytokine production by epithelial cells [18] that can impair AFC by inhibiting ion transporter proteins [21], impair the APP [5], and induce apoptosis of AECs [22]. Previous studies in conjunction with our own have reported attenuation of lung proinflammatory responses

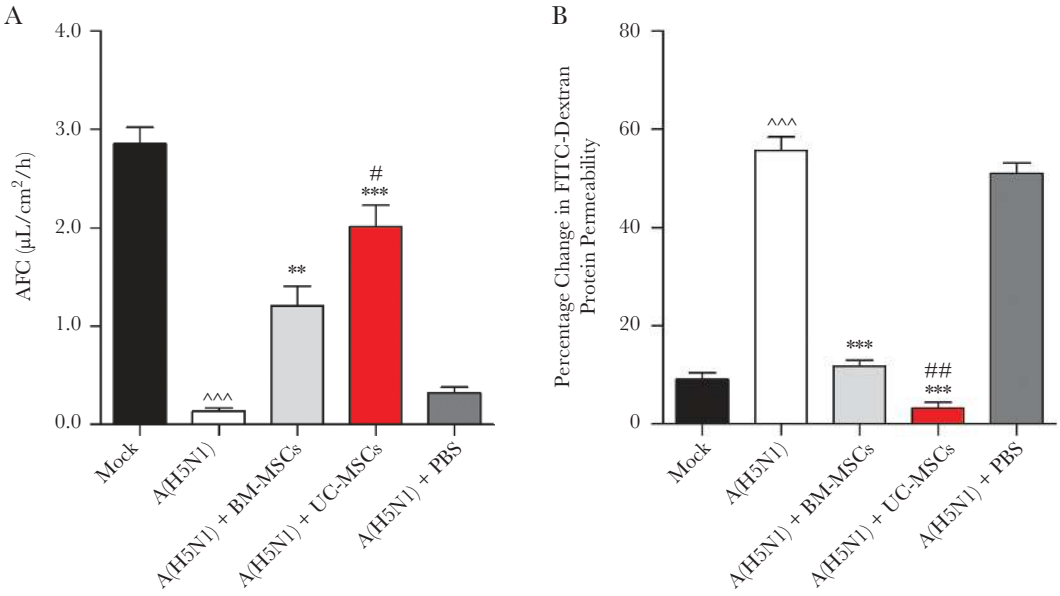

Figure 1. Umbilical cord mesenchymal stromal cells (UC-MSCs) are more effective than bone marrow MSCs (BM-MSCs) in correcting impaired alveolar fluid clearance (AFC) and alveolar protein permeability (APP) of infected alveolar epithelial cells (AECs). AECs in the apical compartment of the Transwell system were infected with influenza A(H5N1) virus (A/HK/483/97) at a multiplicity of infection of 0.1 with small airway epithelial cell growth medium (SAGM), BM-MSCs, UC-MSCs, or phosphate-buffered saline (PBS) in the basal compartment. AFC (*A*) and APP (*B*) were measured 24 hours after infection. Data are representative of 3 independent experiments and plotted as means ± standard errors of the mean. **P* < .05, ***P* < .01, and ****P* < .001, by 1-way analysis of variance with the Bonferroni post hoc test, for comparisons to A(H5N1)-infected AECs alone (*), mock-infected AECs (^), or A(H5N1)-infected AECs with BM-MSCs (#).

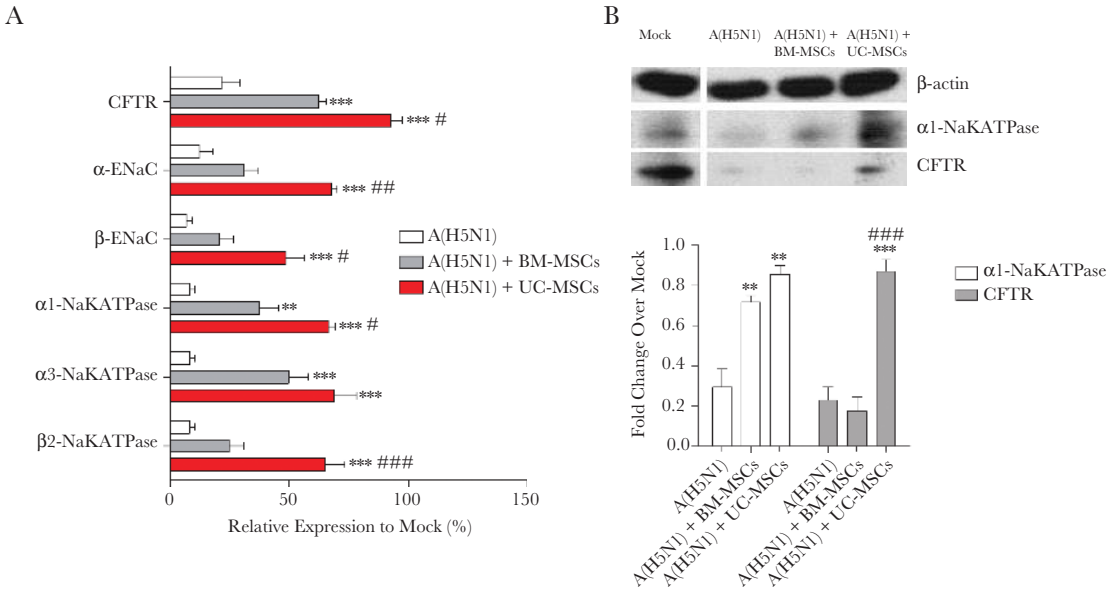

Figure 2. Umbilical cord mesenchymal stromal cells (UC-MSCs) restore influenza A(H5N1) virus–downregulated ion transporter expression in infected alveolar epithelial cells (AECs). *A*, Messenger RNA gene expression of cystic fibrosis transmembrane conductance regulator (CFTR), α-epithelial Na^+ channel (ENaC), β-ENaC, and α1-Na^+K^+ATPase, α2-Na^+K^+ATPase, and β2-Na^+K^+ATPase in AECs 24 hours after infection (multiplicity of infection, 2). *B*, Protein expression of ion transporters 48 hours after infection, as detected by Western blot (top), with corresponding densitometry values (bottom). All data are representative of 3 independent experiments and plotted as means ± standard errors of the mean. **P* < .05, ***P* < .01, and ****P* < .001, by 2-way analysis of variance with the Bonferroni post hoc test, for comparisons to A(H5N1)-infected AECs alone (*) or with bone marrow MSCs (BM-MSCs; #).

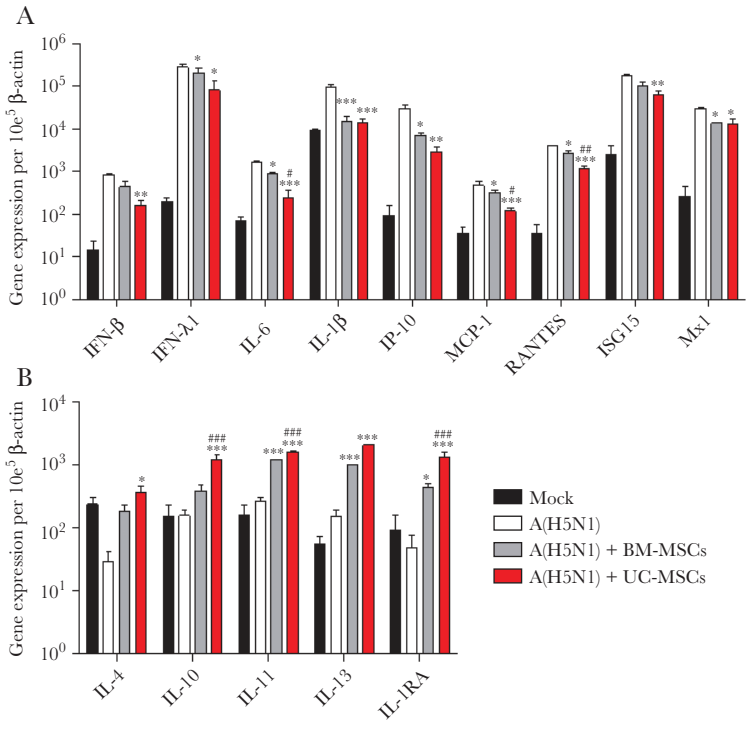

Figure 3. Umbilical cord mesenchymal stromal cell (UC-MSCs) regulate influenza A(H5N1) virus–associated inflammatory responses of epithelial cells. Messenger RNA gene expression of proinflammatory cytokines and chemokines (interferon [IFN] and IFN-related cytokines; *A*) and antiinflammatory cytokines (*B*) in infected alveolar epithelial cells (AECs; multiplicity of infection, 2) 24 hours after infection. All data are plotted as means ± standard errors of the mean and indicative of 3 independent experiments. **P* < .05, ***P* < .01, and ****P* < .001, by 1-way analysis of variance with the Bonferroni post hoc test, for comparisons to A(H5N1)-infected AECs (*) or A(H5N1)-infected AECs with bone marrow MSCs (BM-MSCs; #). IL-1β, interleukin 1β; IL-1RA, interleukin 1 receptor antagonist; IL-4, interleukin 4; IL-6, interleukin 6; IL-10, interleukin 10; IL-11, interleukin 11; IL-13, interleukin 13; IP-10, IFN-γ–induced protein 10; ISG15, IFN-stimulated gene 15; MCP-1, monocyte chemoattractant protein 1; RANTES, regulated on activation normal T-cell expressed and secreted.

by BM-MSCs in ALI [23, 24]. We found that UC-MSCs reduced A(H5N1) induction of several major proinflammatory cytokines in infected AECs: interferon β (IFN-β), IFN-λ1, interleukin 6 (IL-6), interleukin 1β (IL-1β), IFN-γ–induced protein 10 (IP-10), monocyte chemoattractant protein 1 (MCP-1), and regulated on activation normal T-cell expressed and secreted (RANTES), compared with infected AECs alone (Figure 3A). Notably, UC-MSCs reduced IL-6, MCP-1, and RANTES induction more significantly than BM-MSCs. Interestingly, IFN-β induction was only reduced in infected AECs with UC-MSCs.

We also measured gene expression of a panel of the following antiinflammatory cytokines: interleukin 4 (IL-4), interleukin 10 (IL-10), interleukin 11 (IL-11), interleukin 13 (IL-13), and IL-1 receptor antagonist (IL-1RA). Infected AECs with UC-MSCs showed significantly enhanced responses of all antiinflammatory cytokines, compared with AECs alone (Figure 3B). This enhancement was also seen in infected AECs with BM-MSCs, although it was weaker than that for AECs with UC-MSCs. Particularly, UC-MSCs stimulated greater IL-10, IL-11, and IL-RA responses, compared with BM-MSCs.

Conditioned Medium From UC-MSCs Restores A(H5N1)-Impaired AFC and APP

The therapeutic properties of MSCs have been widely attributed to paracrine mechanisms through studies that replace MSCs with their supernatant [21, 25], so we proceeded to test the efficacy of the UC-MSC secretome in the lung injury model. First, UC-MSC supernatant conditioned by A(H5N1)-infected alveolar epithelial cells in the apical compartment was collected and identified as conditioned UC-MSC medium (UC-CdM). In a separate experiment, infected AECs were incubated with UC-CdM in the basal compartment. Similar to previous results, the AFC (Figure 4A) and APP (Figure 4B) of infected AECs were restored by UC-CdM as effectively as its MSC counterpart.

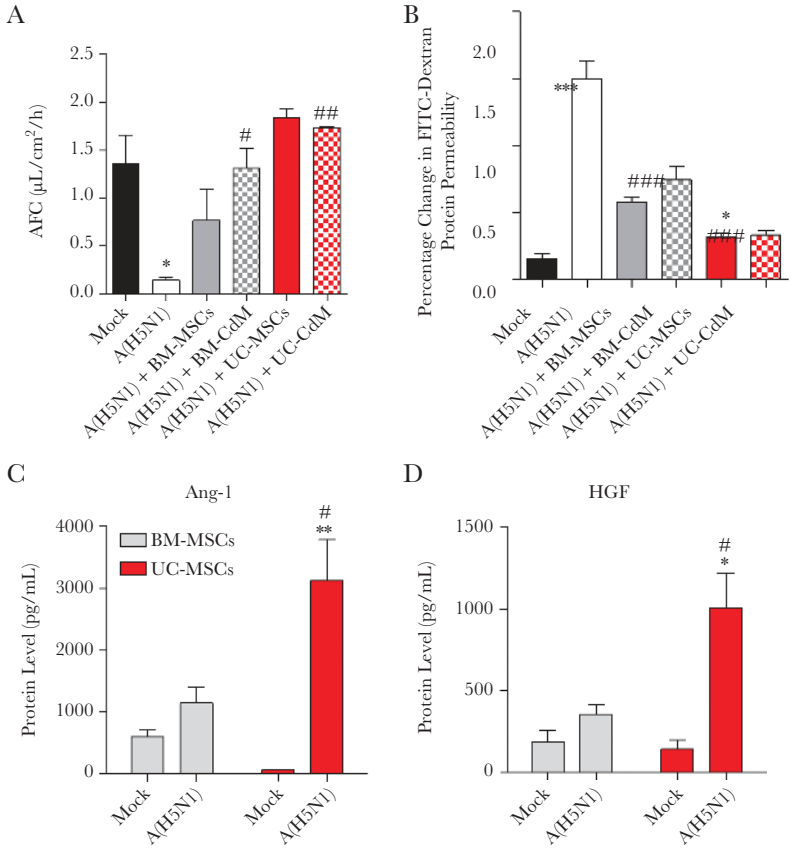

Figure 4. Umbilical cord mesenchymal stromal cell (UC-MSCs) are potent in restoring alveolar fluid clearance (AFC) and alveolar protein permeability (APP) of influenza A(H5N1) virus–infected AECs, partially because of greater angiopoietin 1 (Ang-1) and hepatocyte growth factor (HGF) secretory responses. AECs in the apical compartment of the Transwell system were infected with A/HK/483/97(H5N1) at a multiplicity of infection of 0.1 with small airway epithelial cell growth medium (SAGM), bone marrow MSCs (BM-MSCs), UC-MSCs, conditioned medium from BM-MSCs (BM-CdM) or UC-MSCs (UC-CdM), or phosphate-buffered saline (PBS) control in the basal compartment. *A* and *B*, AFC (*A*) and APP (*B*) was measured 24 hours after infection. Data are representative of 3 independent experiments and expressed as means ± standard errors of the mean (SEMs). $^{*}P < .05$, $^{**}P < .01$, and $^{***}P < .001$, by 1-way analysis of variance with the Bonferroni post hoc test, for comparisons to mock-infected AECs (*), A(H5N1)-infected AECs with no MSC (#), or A(H5N1)-infected AECs with BM-MSC (+). *C* and *D*, Basal MSC supernatant with mock-infected AECs or A(H5N1)-infected AECs on the apical compartment was analyzed for Ang-1 (*C*) and HGF (*D*) by enzyme-linked immunosorbent assay 24 hours after infection. All data are plotted as means ± SEMs and indicative of 3 independent experiments. $^{*}P < .05$, $^{**}P < .01$, and $^{***}P < .001$, by 1-way analysis of variance with the Bonferroni post hoc test, for comparisons to mock (*) or BM-MSC (#).

On the basis of our findings in Figure 1, we also proposed that the UC-MSC secretome would be more potent than that of BM-MSCs in restoring A(H5N1)-impaired AFC and APP. Accordingly, conditioned BM-MSC medium did not perform as well as UC-CdM in correcting the AFC and APP.

We then measured levels of 2 known MSC secretory growth factors involved in epithelial repair, angiopoietin 1 (Ang-1) and hepatocyte growth factor (HGF), in UC-MSC supernatant by an enzyme-linked immunosorbent assay.

Minimal Ang-1 was detected in UC-MSCs with uninfected apical AECs (the mock-infected control), but A(H5N1) infection of AECs stimulated a 49-fold increase of the Ang-1 level (Figure 4C). A similar trend was observed for HGF, whereby higher protein concentration (7-fold) was detected in UC-MSCs incubated with A(H5N1)-infected AECs, compared to uninfected AECs (Figure 4D). When we analyzed BM-MSC supernatant in parallel, we found that, although basal Ang-1 and HGF concentrations were higher in BM-MSCs (the mock-infected control), the fold change increase in response to A(H5N1) infection of AECs was significantly less (2-fold for both Ang-1 and HGF) than that observed in UC-MSCs.

UC-MSCs Restore A(H5N1)-Impaired AFC and APP Partly Through Ang-1 and HGF Secretion

To further elucidate the roles of Ang-1 and HGF, recombinant proteins were used in place of conditioned MSC medium in the in vitro model. Recombinant Ang-1 (rhAng-1) significantly increased AFC, but the increase was less effective than that for UC-MSCs (Figure 5A). The presence of both Ang-1 and HGF was slightly more effective than that of Ang-1 alone, but it was still not comparable to that for UC-MSCs. Interestingly, AFC of infected AECs with recombinant HGF (rhHGF) was the least effective treatment group. rhAng-1 and rhHGF individually restored the A(H5N1)-impaired APP, but the restoration was less effective, compared with UC-MSCs and rhAng-1 and rhHGF together (Figure 5B). The effect of the 2 recombinant proteins together was comparable to that of UC-MSCs in reducing the APP. However, no statistical difference was found between all 4 treatment conditions.

UC-MSCs transfected with Ang-1 or HGF small interfering RNA (siRNA; siAng-1 or siHGF) also restored AFC, but the restoration was less effective than that for UC-MSCs (Figure 5C). Transfection with both siRNA sequences produced the smallest effects on AFC, although this was not statistically different from the A(H5N1) infection condition. For the APP, UC-MSCs transfected with Ang-1 or HGF siRNA still increased the APP, compared with A(H5N1)-infected AECs with no UC-MSCs, and were only slightly less effective than nontransfected UC-MSCs (Figure 5D). However, UC-MSCs transfected with both siAng-1 and siAng-1 only reduced the APP to approximately 50% of the changes induced by A(H5N1), and this was statistically different from the APP measured for all other conditions.

UC-MSC Exosomes Restore A(H5N1)-Impaired AFC and APP

To explore another therapeutic component of UC-MSCs, exosomes were isolated and applied to the in vitro ALI model. UC-MSC exosomes restored the impaired AFC of AECs induced by A(H5N1) infection, but this change was less statistically significant than the restoration by UC-MSCs (Figure 6A). However, exosomes prevented changes in the APP in a fashion similar to that of UC-MSCs (Figure 6B).

Therapeutic Effects of UC-MSCs in A(H5N1)-Induced ALI In Vivo

In light of the promising therapeutic effect of UC-MSCs in restoring AFC and APP in A(H5N1)-infected AECs in vitro, the therapeutic effect of UC-MSCs was studied in a mouse model of A(H5N1)-induced ALI (Figure 7). Young BALB/c mice (age, 6–8 weeks) were challenged with a clinical isolate of A(H5N1) (A/HK/486/97), and 5×10^5 UC-MSCs or fibroblasts were administered intravenously on day 5 after infection. Effects of UC-MSC treatment on survival, body weight, lung alveolar permeability, and cytokine levels were assessed at various times after infection.

Survival began to decline at day 8 and dropped to approximately 30% by day 18 (Figure 7A). Although survival was slightly higher in the UC-MSC treatment group, no statistical significance was found between the UC-MSC and fibroblast groups. On day 18, survival of the UC-MSC treatment group fell to 40%. The slight improvement by UC-MSCs was also reflected by body weight measurements. Body weights of infected mice that received UC-MSC treatment were marginally higher than in the control group and were significantly greater on days 16 and 17 (Figure 7B). The level of Evans blue dye was measured as an indicator of fluid clearance into the alveolar airspace. Lower concentrations of Evans blue dye were found in the lungs of infected mice administered UC-MSCs as compared to fibroblasts, with statistical significant differences on days 10 and 14 (Figure 7C).

Proinflammatory cytokine and chemokine protein levels in bronchoalveolar lavage from A(H5N1)-infected mice with and those without UC-MSC treatment was determined on day 7 after infection. IP-10, MCP-1, RANTES, TNF-α, IL-1β, IL-6, and IL-8 protein levels were all significantly lower in the UC-MSC treatment group, compared with the mouse fibroblast group (Figure 7D). Significance was greatest for IP-10, MCP-1, RANTES, and IL-6.

Lung viral titers were measured on days 7 and 10 to confirm infection and antiviral effects of UC-MSCs. No differences in lung viral titers were detected between UC-MSC and fibroblast treatment groups at either time point (Supplementary Figure 4A). Comparable lung pathology was observed between MSC-treated and untreated mice infected with A(H5N1) (Supplementary Figure 4B).

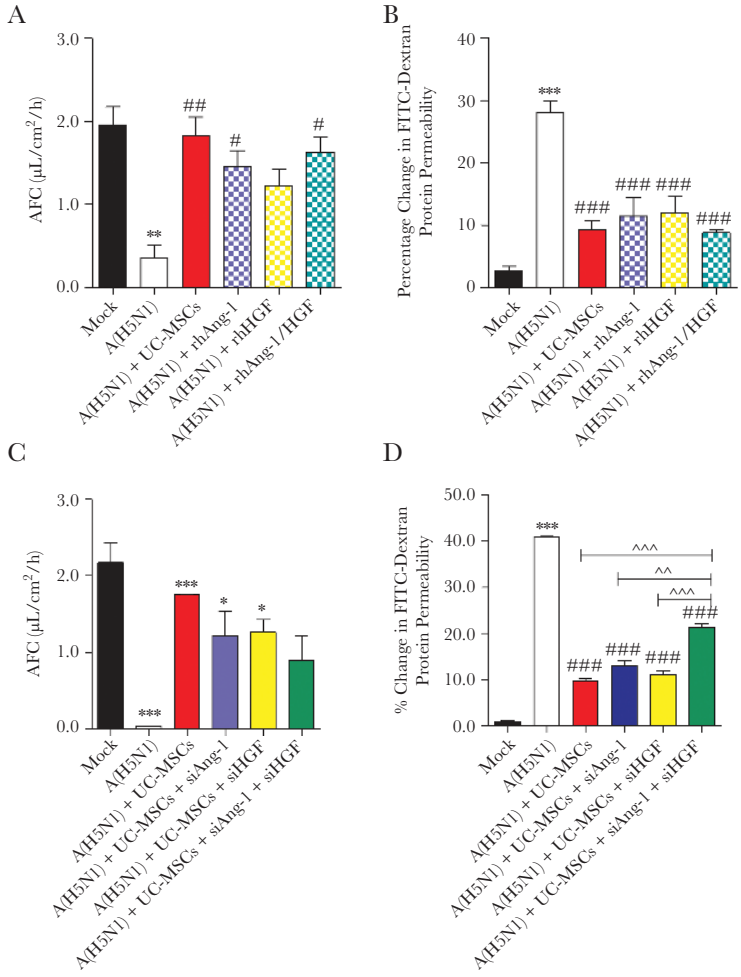

Figure 5. Effects of angiopoietin 1 (Ang-1) and hepatocyte growth factor (HGF) on alveolar fluid clearance (AFC) and alveolar protein permeability (APP) of A(H5N1)-infected alveolar epithelial cells (AECs). AECs in the apical compartment of the Transwell system underwent mock or influenza A/HK/483/97(H5N1) infection at a multiplicity of infection 0.1, with umbilical cord mesenchymal stromal cell (UC-MSCs), recombinant Ang-1 (rhAng-1), HGF (rhHGF), both (rhAng-1/HGF) or UC-MSCs transfected with Ang-1 (siAng-1), HGF (siHGF) or both Ang-1 and HGF (siAng1+siHGF) small interfering RNA (siRNA) in the basal compartment. AFC (*A* and *C*) and APP (*B* and *D*) were measured 24 hours after infection. Data are representative of 3 independent experiments and expressed as means ± standard errors of the mean. **P* < .05, ***P* < .01, ****P* < .001, by 1-way analysis of variance with the Bonferroni post hoc test, for comparisons to mock-infected AECs (*) or A(H5N1)-infected AECs (#).

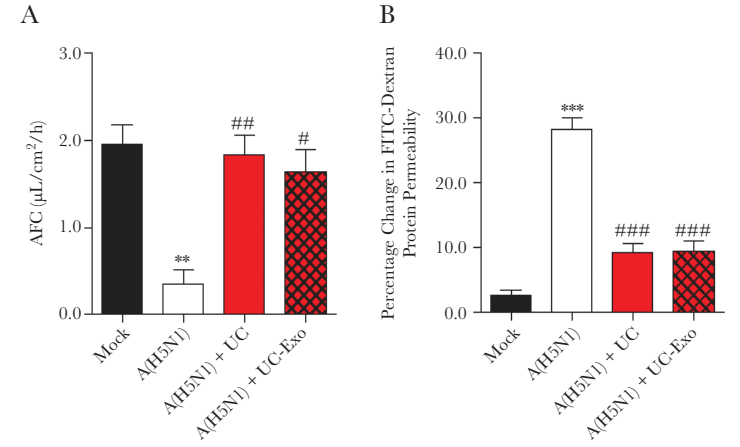

Figure 6. Effects of umbilical cord mesenchymal stromal cell (UC-MSC)–derived exosomes versus UC-MSCs on alveolar fluid clearance (AFC) and alveolar protein permeability (APP) of infected alveolar epithelial cells (AECs). AECs in the apical compartment of the Transwell system underwent mock or influenza A/HK/483/97(H5N1) virus infection at a multiplicity of infection of 0.1 with UC-MSCs or exosomes (UC-Exo) derived from UC-MSCs (UC) in the basal compartment. AFC (*A*) and APP (*B*) were measured 24 hours after infection. Data are representative of 3 independent experiments and expressed as means ± standard errors of the mean. **P* < .05, ***P* < .01, and ****P* < .001, by 1-way analysis of variance with the Bonferroni post hoc test, for comparisons to mock-infected AECs (*) or A(H5N1)-infected AECs (#).

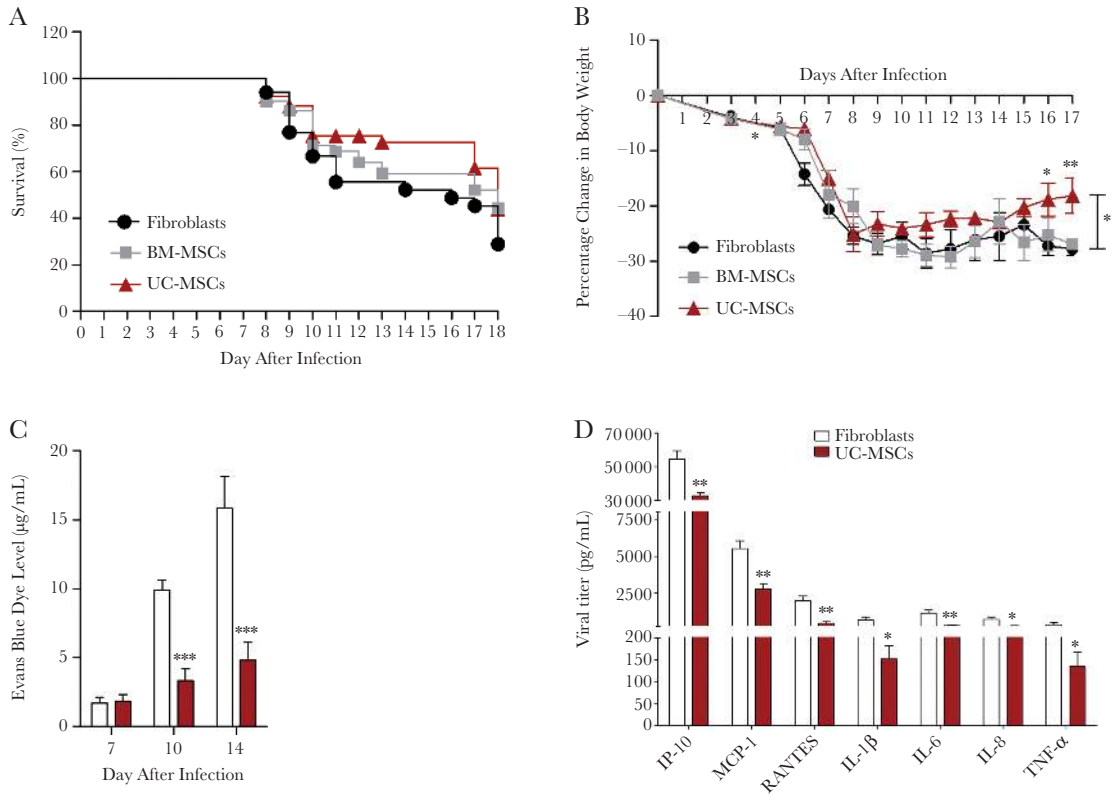

Figure 7. Highly pathogenic influenza model of acute lung injury in young mice. BALB/c mice were inoculated with influenza A(H5N1) virus. Umbilical cord mesenchymal stromal cells (UC-MSCs) or fibroblasts were administered intravenously on day 5. *A* and *B*, Survival (*A*) and body weight (*B*) were monitored until mice were euthanized, on day 18. *C* and *D*, Mice were euthanized at various days for measurement of Evans blue dye extravasation (on days 7, 10, and 14; *C*), viral titers in bronchoalveolar lavage (on day 7; *D*). All data are plotted as means + standard errors of the mean and indicative of 3 data points. * $P < .05$, ** $P < .01$, and *** $P < .001$. BM-MSC, bone marrow MSC; IL-1β, interleukin 1β; IL-6, interleukin 6; IL-8, interleukin 8; IP-10, interferon γ–induced protein 10; MCP-1, monocyte chemoattractant protein 1; RANTES, regulated on activation normal T-cell expressed and secreted; TNF-α, tumor necrosis factor α.

DISCUSSION

In this study, we demonstrated that UC-MSCs are effective in restoring an impaired AFC, APP and major epithelial ion transporter expression of A(H5N1)-infected AECs in vitro, partly through immunomodulation and potent secretion of Ang-1 and HGF. Moreover, UC-MSCs consistently outperformed BM-MSCs, which have many limitations in respect to clinical application, further highlighting the potential of UC-MSCs as a novel therapeutic option for the treatment of influenza-associated ALI.

UC-MSCs have many practical advantages, such as high proliferation rates, that enable robust in vitro culture to obtain numbers sufficient for clinical use. As such, in vivo studies have shown that UC-MSCs reduce bleomycin-induced [26], prenatal [27], and lipopolysaccharide-induced lung injury [28]. However, comparison studies of different types of MSCs in human lung disease models are lacking. Here we have used an adult and perinatal source of MSC in parallel, using an in vitro model, first to directly compare their therapeutic efficacy and second to elucidate mechanistic differences between the action of BM-MSCs and UC-MSCs in ALI.

Cytokines can compromise AFC by inhibiting ion transporter proteins [16, 30] and APP by damaging tight junctions or inducing apoptosis of infected epithelial cells. Therefore, strong immunomodulatory capacities of UC-MSCs are likely central to their role in repairing the A(H5N1)-injured alveolar epithelium. UC-MSCs effectively reduced expression of a panel of major proinflammatory cytokines associated with A(H5N1) infection and, as expected, to a greater extent than BM-MSCs. Superior immunosuppressive capacities of UC-MSCs have mostly been shown by interaction with host immune cells, whether in animals or mixed lymphocyte reactions [11, 13]. Our in vitro model demonstrates that UC-MSCs have a greater intrinsic ability to simply sense and regulate cytokines in their microenvironment. Furthermore, in AECs infected with BM-MSCs and UC-MSCs, we found upregulated levels of genes encoding antiinflammatory interleukins that were not previously studied. In particular, UC-MSCs enhanced IL-10, IL-11, and IL-1RA responses, compared with BM-MSCs, all of whose beneficial roles in lung injury have been established [29–31]. Gene expression analyses have shown that BM-MSCs tend to express more genes involved in osteogenesis, whereas UC-MSCs show

higher expression of genes involved in angiogenesis and matrix remodeling [32], reflecting the function of their respective sites of origin, and may explain why UC-MSCs are a better candidate in wound healing and treatment of inflammatory diseases for which immunosuppressive action is required [33].

Some studies suggest that highly pathogenic viruses can also compromise epithelial permeability by directly damaging tight junctions [34]. The slightly lower expression of the influenza virus matrix gene detected in infected AECs with UC-MSCs suggests that they may have some intrinsic antiviral activity that BM-MSCs lack. The role of MSCs in suppressing host viral infection has not been well studied, although paracrine antiviral activity of UC-MSCs has been reported for hepatitis C virus through secretion of specific miRNA sequences [35].

As UC-MSCs are of neonatal origin, they are more primitive than adult-tissue-derived BM-MSCs and so may exert bigger responses to injurious stimuli. We observed that UC-MSCs showed greater secretion of 2 paracrine soluble factors—Ang-1 and HGF—upon infection, compared with BM-MSCs. Ang-1 is a Tie2 receptor ligand involved in angiogenesis that restores alveolar epithelial permeability in ALI by upregulating tight-junction claudin 18 [19]. However, we have previously shown that BM-MSC–secreted Ang-1 only partially accounts for the therapeutic effect of MSCs on AFC and APP, so we also studied another major MSC secretory protein. HGF is a pulmotrophic factor that regulates cell growth, motility, and morphogenesis by binding to the c-Met receptor and has been shown to inhibit epithelial apoptosis [36]. More recently, it was reported to restore lung permeability by protecting tight junctions and inhibiting endothelial apoptosis in a bacterial ALI model [37]. Therefore, higher concentrations of Ang-1, HGF and other paracrine factors may also explain why UC-MSCs were more effective in correcting AFC and APP. Ang-1 and HGF are both important in accounting for the restorative effects of UC-MSCs on AFC and APP in A(H5N1)-induced ALI in vitro.

Previous in vivo studies in conjunction with our own have found that BM-MSCs failed to improve survival of young mice (age, 6–8 weeks) inoculated with A(H1N1), 2009 pandemic A(H1N1), or A(H5N1) and that MSC treatment was only beneficial to older mice (age, 8–12 months), reflecting age-related differences in mechanisms of lung pathology and repair [38]. Thus, we reasoned that neonatal UC-MSCs, whose functions are not limited by age, would more therapeutically potent than BM-MSCs and perform better in young mice with influenza-associated ALI. However, the therapeutic benefits of UC-MSCs in mice shown here are only marginal, prompting several improvements of the current in vivo model that could be made, including optimization of the UC-MSC dosage, frequency of administration, and delivery route.

Emerging studies have shown that BM-MSCs can alleviate ALI by secreting extracellular vesicles that carry reparative protein and RNA (eg, mRNA and miRNA) to injured cells [39]. Thus, we isolated exosomes, the smallest known type of extracellular vesicle and applied it first to our in vitro model in direct comparison with UC-MSCs. Our data show that exosomes derived from UC-MSCs are as potent in restoring AFC and APP as their parent cells, suggesting that exosomes are an alternative therapy to UC-MSCs. It would also be interesting to explore different administration methods for exosomes, as they have potential for aerosol delivery.

In conclusion, our data show that UC-MSCs, in addition to their constituents, such as conditioned medium, specific secretory growth factors, and exosomes, are potent attenuators of A(H5N1)-associated ALI and may offer a promising therapeutic alternative to conventionally used BM-MSCs in establishing improved preclinical models for severe human influenza.

Supplementary Data

Supplementary materials are available at *The Journal of Infectious Diseases* online. Consisting of data provided by the authors to benefit the reader, the posted materials are not copyedited and are the sole responsibility of the authors, so questions or comments should be addressed to the corresponding author.

Notes

Acknowledgments. We thank Mandy M. T. Ng, Man Chun Cheung, Hung Sing Li, and Rachel H. H. Ching at the School of Public Health, LKS Faculty of Medicine, University of Hong Kong, for technical support; and Kevin Fung at the Department of Pathology, University of Hong Kong, for immunohistochemical staining.

Financial support. This work was supported by the National Institute of Allergy and Infectious Diseases (grant HHSN272201400006C); the Research Grants Council of the Hong Kong Special Administrative Region, People's Republic of China (T11-705/14N); and the Innovation and Technology Commission (reference UIM/212).

Potential conflicts of interest. All authors: No reported conflicts of interest. All authors have submitted the ICMJE Form for Disclosure of Potential Conflicts of Interest. Conflicts that the editors consider relevant to the content of the manuscript have been disclosed.

References

1. Short KR, Kroeze EJBV, Fouchier RAM, Kuiken T. Pathogenesis of influenza-induced acute respiratory distress syndrome. Lancet Infect Dis **2014**; 14:57–69.
2. Fronius M, Clauss WG, Althaus M. Why do we have to move fluid to be able to breathe? Front Physiol **2012**; 3:146.
3. Matthay MA. Resolution of pulmonary edema. Thirty years of progress. Am J Respir Crit Care Med **2014**; 189:1301–8.
4. Antunes MA, Laffey JG, Pelosi P, Rocco PR. Mesenchymal stem cell trials for pulmonary diseases. J Cell Biochem **2014**; 115:1023–32.

5. Chan MC, Kuok DI, Leung CY, et al. Human mesenchymal stromal cells reduce influenza A H5N1-associated acute lung injury in vitro and in vivo. Proc Natl Acad Sci U S A **2016**; 113:3621–6.
6. Huppert LA, Matthay MA. Alveolar fluid clearance in pathologically relevant conditions: in vitro and in vivo models of acute respiratory distress syndrome. Front Immunol **2017**; 8:371.
7. Bustos ML, Huleihel L, Kapetanaki MG, et al. Aging mesenchymal stem cells fail to protect because of impaired migration and antiinflammatory response. Am J Respir Crit Care Med **2014**; 189:787–98.
8. Lu LL, Liu YJ, Yang SG, et al. Isolation and characterization of human umbilical cord mesenchymal stem cells with hematopoiesis-supportive function and other potentials. Haematologica **2006**; 91:1017–26.
9. Nazarov I, Lee JW, Soupene E, et al. Multipotent stromal stem cells from human placenta demonstrate high therapeutic potential. Stem Cells Transl Med **2012**; 1:359–72.
10. Li X, Bai J, Ji X, Li R, Xuan Y, Wang Y. Comprehensive characterization of four different populations of human mesenchymal stem cells as regards their immune properties, proliferation and differentiation. Int J Mol Med **2014**; 34:695–704.
11. Prasanna SJ, Gopalakrishnan D, Shankar SR, Vasandan AB. Pro-inflammatory cytokines, IFNgamma and TNFalpha, influence immune properties of human bone marrow and Wharton jelly mesenchymal stem cells differentially. PLoS One **2010**; 5:e9016.
12. Amable PR, Teixeira MV, Carias RB, Granjeiro JM, Borojevic R. Protein synthesis and secretion in human mesenchymal cells derived from bone marrow, adipose tissue and Wharton's jelly. Stem Cell Res Ther **2014**; 5:53.
13. Bárcia RN, Santos JM, Filipe M, et al. What makes umbilical cord tissue-derived mesenchymal stromal cells superior immunomodulators when compared to bone marrow derived mesenchymal stromal cells? Stem Cells Int **2015**; 2015:583984.
14. Cruz FF, Borg ZD, Goodwin M, et al. Systemic administration of human bone marrow-derived mesenchymal stromal cell extracellular vesicles ameliorates aspergillus hyphal extract-induced allergic airway inflammation in immunocompetent mice. Stem Cells Transl Med **2015**; 4:1302–16.
15. Phinney DG, Di Giuseppe M, Njah J, et al. Mesenchymal stem cells use extracellular vesicles to outsource mitophagy and shuttle microRNAs. Nat Commun **2015**; 6:8472.
16. Lee C, Mitsialis SA, Aslam M, et al. Exosomes mediate the cytoprotective action of mesenchymal stromal cells on hypoxia-induced pulmonary hypertension. Circulation **2012**; 126:2601.
17. Khatri M, Richardson LA, Meulia T. Mesenchymal stem cell-derived extracellular vesicles attenuate influenza virus-induced acute lung injury in a pig model. Stem Cell Res Ther **2018**; 9:17.
18. Chan MC, Cheung CY, Chui WH, et al. Proinflammatory cytokine responses induced by influenza A (H5N1) viruses in primary human alveolar and bronchial epithelial cells. Respir Res **2005**; 6:135.
19. Fang X, Neyrinck AP, Matthay MA, Lee JW. Allogeneic human mesenchymal stem cells restore epithelial protein permeability in cultured human alveolar type II cells by secretion of angiopoietin-1. J Biol Chem **2010**; 285:26211–22.
20. Sartori C, Matthay MA. Alveolar epithelial fluid transport in acute lung injury: new insights. Eur Respir J **2002**; 20:1299–313.
21. Goolaerts A, Pellan-Randrianarison N, Larghero J, et al. Conditioned media from mesenchymal stromal cells restore sodium transport and preserve epithelial permeability in an in vitro model of acute alveolar injury. Am J Physiol Lung Cell Mol Physiol **2014**; 306:L975–85.
22. Hui KP, Li HS, Cheung MC, et al. Highly pathogenic avian influenza H5N1 virus delays apoptotic responses via activation of STAT3. Sci Rep **2016**; 6:28593.
23. Curley GF, Ansari B, Hayes M, et al. Effects of intratracheal mesenchymal stromal cell therapy during recovery and resolution after ventilator-induced lung injury. Anesthesiology **2013**; 118:924–32.
24. Danchuk S, Ylostalo JH, Hossain F, et al. Human multipotent stromal cells attenuate lipopolysaccharide-induced acute lung injury in mice via secretion of tumor necrosis factor-α-induced protein 6. Stem Cell Res Ther **2011**; 2:27.
25. Ionescu L, Byrne RN, van Haaften T, et al. Stem cell conditioned medium improves acute lung injury in mice: in vivo evidence for stem cell paracrine action. Am J Physiol Lung Cell Mol Physiol **2012**; 303:L967–77.
26. Moodley Y, Atienza D, Manuelpillai U, et al. Human umbilical cord mesenchymal stem cells reduce fibrosis of bleomycin-induced lung injury. Am J Pathol **2009**; 175:303–13.
27. Liu QP, Zhou DX, Sun L, et al. Bone marrow mesenchymal stem cells ameliorates seawater-exposure-induced acute lung injury by inhibiting autophagy in lung tissue. Patholog Res Int **2014**; 2014:104962.
28. Zhu H, Xiong Y, Xia Y, et al. Therapeutic effects of human umbilical cord-derived mesenchymal stem cells in acute lung injury mice. Sci Rep **2017**; 7:39889.
29. Ortiz LA, Dutreil M, Fattman C, et al. Interleukin 1 receptor antagonist mediates the antiinflammatory and antifibrotic effect of mesenchymal stem cells during lung injury. Proc Natl Acad Sci U S A **2007**; 104:11002–7.
30. Sheridan BC, Dinarello CA, Meldrum DR, Fullerton DA, Selzman CH, McIntyre RC Jr. Interleukin-11 attenuates

pulmonary inflammation and vasomotor dysfunction in endotoxin-induced lung injury. Am J Physiol **1999**; 277:L861–7.
31. Inoue G. Effect of interleukin-10 (IL-10) on experimental LPS-induced acute lung injury. J Infect Chemother **2000**; 6:51–60.
32. Panepucci RA, Siufi JL, Silva WA Jr, et al. Comparison of gene expression of umbilical cord vein and bone marrow-derived mesenchymal stem cells. Stem Cells **2004**; 22:1263–78.
33. Santos JM, Bárcia RN, Simões SI, et al. The role of human umbilical cord tissue-derived mesenchymal stromal cells (UCX®) in the treatment of inflammatory arthritis. J Transl Med **2013**; 11:18.
34. Golebiewski L, Liu H, Javier RT, Rice AP. The avian influenza virus NS1 ESEV PDZ binding motif associates with Dlg1 and Scribble to disrupt cellular tight junctions. J Virol **2011**; 85:10639–48.
35. Zhao Y, Sun X, Cao W, et al. Exosomes derived from human umbilical cord mesenchymal stem cells relieve acute myocardial ischemic injury. Stem Cells Int **2015**; 2015:761643.
36. Okada M, Sugita K, Inukai T, et al. Hepatocyte growth factor protects small airway epithelial cells from apoptosis induced by tumor necrosis factor-alpha or oxidative stress. Pediatr Res **2004**; 56:336–44.
37. Hu S, Li J, Xu X, et al. The hepatocyte growth factor-expressing character is required for mesenchymal stem cells to protect the lung injured by lipopolysaccharide in vivo. Stem Cell Res Ther **2016**; 7:66.
38. Gotts JE, Abbott J, Matthay MA. Influenza causes prolonged disruption of the alveolar-capillary barrier in mice unresponsive to mesenchymal stem cell therapy. Am J Physiol Lung Cell Mol Physiol **2014**; 307:L395–406.
39. Zhu YG, Feng XM, Abbott J, et al. Human mesenchymal stem cell microvesicles for treatment of *Escherichia coli* endotoxin-induced acute lung injury in mice. Stem Cells **2014**; 32:116–25.